

# Phyllosilicate-like structure anchored silylating agents: calorimetric data on divalent cation–aminated centre interactions in the lamellar cavity

Maria G. da Fonseca and Claudio Airoidi\*

*Instituto de Química, Universidade Estadual de Campinas, Caixa Postal 6154, 13083-970 Campinas, São Paulo, Brasil*

*Received 15th July 1999, Accepted 9th September 1999*

Nanocomposites with phyllosilicate-like structure containing silylating agents have been synthesized by using metal ions to aid the formation of the inorganic matrix, giving a structure similar to that of talc. Two distinct silicates were prepared by treating magnesium chloride with 3-aminopropyltrimethoxysilane or 6-amino-4-azahexyltrimethoxysilane, catalysed by sodium hydroxide, to give SILMg1 and SILMg2, with lamellar distances of 1731 and 2053 pm, respectively. Adsorption isotherms were obtained by suspending the solid with  $M(\text{NO}_3)_2$  solutions ( $M = \text{Cu}, \text{Zn}, \text{Ni}$  or  $\text{Co}$ ), which gave the number of moles adsorbed as  $7.70 \pm 0.050$ ,  $6.10 \pm 0.04$  and  $3.81 \pm 0.01$ ,  $2.20 \pm 0.01$   $\text{mmol g}^{-1}$  for SILMg1 and SILMg2 with  $\text{Cu}^{2+}$  and  $\text{Zn}^{2+}$ , respectively. These data obtained from a batch method were adjusted to the Langmuir model. The adsorption process was also followed by microcalorimetry, by suspending the mass of material in 2.0  $\text{cm}^3$  of water and titrating with aqueous solutions of the cations. From these values, the respective thermal effects of dilution were subtracted to give the net thermal effects, which enabled the determination of  $\Delta H$  and  $K$  values and from them  $\Delta G$  and  $\Delta S$  values. The exothermic enthalpic values for  $\text{Cu}^{2+}$ ,  $\text{Zn}^{2+}$ ,  $\text{Ni}^{2+}$  and  $\text{Co}^{2+}$  were  $-8.62 \pm 0.56$ ,  $-8.20 \pm 0.48$ ,  $-3.78 \pm 0.03$  and  $8.86 \pm 0.81$  for SILMg1 and  $-8.40 \pm 0.50$ ,  $-9.29 \pm 0.55$ ,  $-20.12 \pm 0.67$  and  $-61.55 \pm 0.06$  for SILMg2. The entropic values varied from 27 to 143  $\text{J K}^{-1} \text{mol}^{-1}$ . The exothermic values for all free energies indicated that the cations are favourably bonded to the pendant groups disposed in the lamellar cavities.

Clay minerals have been extensively studied due to their properties associated with chemical intercalation and also to some characteristics of their surfaces. Among those minerals, the well known phyllosilicates found in soils and sediments such as smectites constitute a class of inorganic catalysts. However, the interest in synthetic minerals has been increased since some of them can be obtained with defined chemical composition, crystalline or with structures containing defects, which can be used in many catalytic processes.<sup>1</sup>

The natural clay minerals can be chemically modified through two distinct routes: (i) intercalating organic molecules or (ii) cation exchanging into the interlamellar space. The first route enables immobilization of catalysts in the structure of the minerals, such as some complexes that act as homogeneous catalysts. This procedure opened the possibility to follow selected reactions in the solid state, in order to simulate the ones observed in solution. This synthetic procedure minimized many technical and technological barriers associated with the use of these complexes as homogeneous catalysts. However, more recently, organic modified phyllosilicates have been obtained through the sol–gel process. This allows the insertion of organic molecules into an inorganic matrix, originating pure inorganic–organic hybrids, in a homogeneous way and with controlled porosity. By employing this route, some phyllosilicates have been prepared by copolymerization of metal ions with a set of trialkoxysilanes.<sup>2–7</sup> Those nanocomposites present some advantages over the natural ones, because the obtained compound can also be chemically modified in subsequent stages. Other features associated to the synthetic procedure are related to the ability to obtain pure chemical composition or defects in the final compounds. In this last case, the vacancy can be exploited as a specific function in the structure.

This publication reports a synthetic method for modified phyllosilicates by using a metal ion, for instance magnesium, and two aminated alkoxy-silanes, such as amino-

propyltrimethoxysilane and 6-amino-4-azahexyltrimethoxysilane, yielding the products SILMg1 and SILMg2, respectively. From the structural point of view, these polymeric lamellar nanocomposites are formed by an inorganic sheet containing magnesium atom octahedrally co-ordinated by oxygen atoms, which are shared with silicon atoms in a tetrahedral coordination. To this structure, chains of organic moieties are bonded to the inorganic matrix by using one co-ordination site of each silicon atom. This general expected lamellar structure is similar to that of natural talc, where two tetrahedral layers of silicon are located between the octahedral layers of magnesium. So, the final synthesized nanocomposites present an organic chain attached to the tetrahedral layers, through silicon–carbon covalent bonding, as represented in Fig. 1. As expected, in varying the length of the pendant organic group R, distinct lamellar distances can be obtained.

Modified surfaces containing nitrogen basic centres attached to the pendant organic chain can potentially possess great ability in extracting metal cations from aqueous and non-aqueous solutions.<sup>8–10</sup> Thus, the interactive effect in the solid/liquid interface is explored to obtain information about the adsorption capacity of some divalent cations. Data were collected from a suspension of the phyllosilicate through the batch method and calorimetric titration in an aqueous medium, which enabled the acquisition of thermodynamic values by using a previous procedure.<sup>11</sup>

## Experimental

### Chemicals

The silylating agents 3-aminopropyltrimethoxysilane and 6-amino-4-azahexyltrimethoxysilane (Aldrich), magnesium chloride hexahydrate (Fluka), methanol and sodium hydroxide (Merck) of reagent grade were used without further purifi-

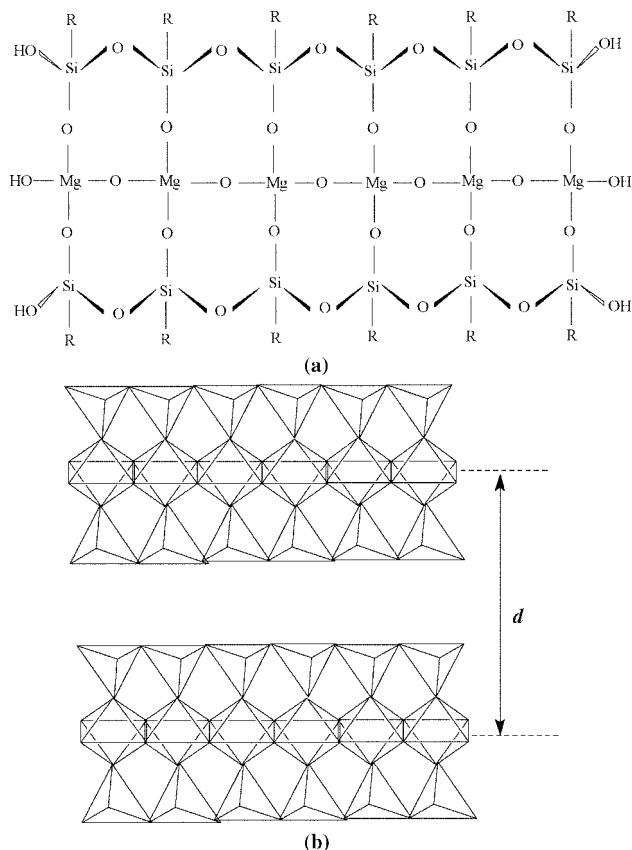


**Fig. 1** Structures of the nanocomposites, where R = CH<sub>2</sub>CH<sub>2</sub>-CH<sub>2</sub>NH<sub>2</sub> on SILMg1 and CH<sub>2</sub>CH<sub>2</sub>CH<sub>2</sub>NHCH<sub>2</sub>CH<sub>2</sub>NH<sub>2</sub> on SILMg2.

cation. Hydrated divalent copper (Merck), nickel (Nuclear) and zinc (Nuclear) nitrates were also used without purification. Bidistilled water was used in all experimental procedures.

#### Synthesis of aminated magnesium phyllosilicates

The first step of this synthetic method consisted in dissolving 0.052 mol of hexahydrated magnesium chloride in 300 cm<sup>3</sup> of bidistilled water and stirring while heating at 373 K. In the next stage, a methanol solution of 1.39 mol dm<sup>-3</sup> of the desired silane dissolved was slowly added. This gives a Si:Mg molar ratio of 1.33:1, as found in natural talc. Immediately, a white suspension appeared and 500.0 cm<sup>3</sup> of an aqueous solution of 0.10 mol dm<sup>-3</sup> sodium hydroxide were slowly added with stirring while maintaining the heating. This last suspension was aged for 5 d at 323 K, giving a gel that was centrifuged, washed with water and dried at 323 K for 5 d. A brittle mass of 15.0 g was formed, which after pulverizing resulted in a white powder.

#### Characterization

X-Ray powder patterns were obtained with nickel-filtered Cu-K $\alpha$  radiation on a Shimadzu model XD3A diffractometer (30/20 kV/mA) and 3.33° s<sup>-1</sup>. Infrared spectra were obtained by using a Perkin-Elmer model 1600 FTIR spectrophotometer on KBr pressed pellets, with 4 cm<sup>-1</sup> resolution. The nuclear magnetic resonance spectra of the solid materials were obtained on an AC 300/P Bruker spectrometer at room temperature at 75.5 and 59.6 MHz for carbon and silicon, respectively. For carbon CP/MAS the spectra were obtained with a pulse repetition time of 3 s and contact time of 3 ms. The results showed that the structure of the organic chain of the silylating agent bonded to the backbone of the layered silicates did not change during the synthetic route employed. The presence of unhydrolysed methoxy groups originating from the silylating agent was not

**Table 1** Percentages (%) of hydrogen, carbon and nitrogen, C:N ratio observed (calculated) and *n* the number of pendant groups on the hybrids (mmol g<sup>-1</sup>)

Hybrid	H	C	N	C:N	<i>n</i>
SILMg1	5.30	15.18	4.94	3.10 (3.10)	3.60
SILMg2	5.76	18.28	7.33	2.49 (2.50)	2.62

detected, thus for O-CH<sub>3</sub> a signal is expected to appear around  $\delta$  50.

For <sup>29</sup>Si NMR spectra the high-power proton decoupling (HPDEC) technique was employed with a pulse repetition time of 60 s, width 45° and spinning speed 4 kHz. The presence of three signals around  $\delta$  -67, -55 and -48 associated to silicon species RSi(OSi)<sub>*n*</sub>(OH)<sub>3-*n*</sub> for *n*=3 to 1 respectively, was detected for the hybrids.

Thermogravimetric curves were obtained by using a DuPont model 1090 B apparatus coupled with a thermobalance 951, on heating from room temperature to 1273 K at a rate of 0.16 K s<sup>-1</sup> in an argon flow rate of 1.66 cm<sup>3</sup> s<sup>-1</sup>. The samples varied in weight from 15.0 to 30.0 mg. Surface area measurements were made on a Flowsorb II 2300 Micromeritics instrument, by applying the Brunauer-Emmett-Teller (BET) equation. Carbon, nitrogen and hydrogen contents were determined by using a Perkin-Elmer microelemental analyser.

#### Adsorption of cations

The batch method was used for adsorption of cations in an aqueous medium containing the phyllosilicate. Samples of approximately 20 mg of the solid were suspended in 25.0 cm<sup>3</sup> of aqueous solutions containing divalent cations in increasing concentrations, varying from 1.0 × 10<sup>-4</sup> to 0.14 mol dm<sup>-3</sup>. The suspension was mechanically stirred on a thermostatted bath at 298 ± 1 K. Based on the time required to reach equilibrium, which was established as less than 3 h, for all experiments 4 h was chosen to ensure maximum extraction. For each point of the isotherm at least two aliquots of 0.50 cm<sup>3</sup> were removed from the supernatant and the amount of the remaining metal was determined by conventional complexometric titration method with standard EDTA solution.<sup>12</sup>

#### Calorimetric titration

The thermal effects of the chemisorption of metallic cations by phyllosilicate were followed in an isothermic LKB 2277 microcalorimetric system, as previously described.<sup>12</sup> A sample of approximately 20 mg was suspended in 2.0 cm<sup>3</sup> of water and vigorously stirred at 298.15 ± 0.02 K. After equilibrium, a solution of a metal cation was added through a microsyringe. For each increment of solution the thermal effect ( $\Sigma\Delta h_{\text{tit}}$ ) was recorded until saturation was reached, indicated by a constant thermal effect. Identically, were monitored the titration of the cation solution in water ( $\Sigma\Delta h_{\text{ait}}$ ) without the solid and also of solid suspended in the water, where hydration of the inorganic-organic hybrid gave a null value. By combining those two thermal effect values the resulting integral thermal effect ( $\Sigma\Delta h_r$ ) can be determined by the expression  $\Sigma\Delta h_r = \Sigma\Delta h_{\text{tit}} - \Sigma\Delta h_{\text{ait}}$ . The change in enthalpy associated to the cation-matrix interaction ( $\Delta h_{\text{int}}$ ) can be determined by adjusting the adsorption data to a modified Langmuir equation.<sup>11,12</sup>

#### Results and discussion

The elemental analyses of the nanocomposites SILMg1 and SILMg2 are listed in Table 1. Based on the nitrogen content determined, there are 3.60 and 2.62 mmol g<sup>-1</sup> of aminated organic groups attached in SILMg1 and SILMg2, respectively. The hybrids were characterized by infrared spectroscopy and showed very similar spectra for both, presenting the bands at

**Table 2** Number of moles of the cations adsorbed ( $N_f$ ), maximum amount of cations adsorbed per mol of hybrids ( $N_s$ ) and coefficient of correlation ( $r$ )

Hybrid	M <sup>2+</sup>	$N_f/\text{mmol g}^{-1}$	$N_s/\text{mmol g}^{-1}$	$r$
SILMg1	Cu <sup>2+</sup>	7.70 ± 0.05	8.09 ± 0.48	0.998
	Zn <sup>2+</sup>	6.10 ± 0.04	6.49 ± 0.13	0.999
	Ni <sup>2+</sup>	5.51 ± 0.04	5.55 ± 0.02	0.999
	Co <sup>2+</sup>	0.40 ± 0.01	0.42 ± 0.02	0.993
SILMg2	Cu <sup>2+</sup>	3.81 ± 0.01	4.53 ± 0.12	0.998
	Zn <sup>2+</sup>	2.20 ± 0.01	2.41 ± 0.05	0.999
	Ni <sup>2+</sup>	3.22 ± 0.05	3.39 ± 0.06	0.999
	Co <sup>2+</sup>	1.07 ± 0.01	1.23 ± 0.04	0.997

2940 [ $\delta(\text{C-H})$ ], 1570 [ $\nu(\text{N-H})$ ], 1450 [ $\nu(\text{CH}_2)$ ], 1320 [ $\delta(\text{N-C})$ ], 1180 [ $\delta(\text{Si-C})$ ], 1010 [ $\nu(\text{Si}_2\text{O}_5)$ ], 800 [ $\nu(\text{N-H})$ ] out of the plane and at 540  $\text{cm}^{-1}$  [ $\nu(\text{Mg-O})$ ]. This last band is a fingerprint of natural silicates such as talc.<sup>13-15</sup> On the other hand, the existence of the same band in all nanocomposites can evidence the presence of the phyllosilicate-like structure.

The crystallinity of these hybrids, analysed by X-ray diffractometry, is quite interesting. Thus, the lamellar peaks of the phyllosilicates correspond to interlamellar distances of 1731 and 2053 pm for SILMgx ( $x = 1$  or 2). These values contrast with that of 934 pm found for the natural phyllosilicate talc whose structure is similar to those obtained here. On the other hand, the diffraction patterns of these hybrids did not show any signal which could be related to the presence of  $\text{Mg}(\text{OH})_2$ . In addition, other well characterized peaks should be displayed at 477 ( $2\theta = 18.6$ ) and 237 pm ( $2\theta = 38.0^\circ$ ) due to 001 and 101 reflections.<sup>16</sup> The largest values observed for the lamellar distances in the synthetic hybrids are, therefore, influenced by the presence of the organic radical chain disposed into the cavity of these structures. As determined previously,<sup>17</sup> the increase in the length of the organic chain of a given radical covalently attached to the inorganic matrix caused an increase in the lamellar distance from SILMg1 to SILMg2. The length of the pendant organic chains in SILMgx was estimated by using a bond distance model, assuming a zigzag conformation of these chains. Thus, the length of the free chain in the gallery space was calculated as 543 and 939 pm for the organic radicals  $(\text{CH}_2)_3\text{NH}_2$  and  $(\text{CH}_2)_3\text{NH}(\text{CH}_2)_2\text{NH}_2$  attached to the inorganic backbone, as was observed before for such hybrids.<sup>17</sup>

The interactions of cations with both phyllosilicates caused a change in the X-ray diffractograms, as is illustrated in Fig. 2. There is an enhancement of the crystallinity of the hybrids when metallic cations are adsorbed, mainly in the case of copper. The interlayer  $d$  value corresponding to the first peak of the diffractogram changed from 670 to 710 pm for SILMg1/ $\text{Cu}^{2+}$ , 680 to 710 pm for SILMg2/ $\text{Cu}^{2+}$  and 825 to 1030 pm for SILMg2/ $\text{Zn}^{2+}$ . On the other hand, nickel cation resulted in an identical interlayer distance of 800 pm for both nanocomposites. The decrease of the original lamellar distance of both hybrids seems to be associated to the conformation of the complex formed with the basic centres of the aminated chains, the chains being brought closer together due to the co-ordination to the cations, as proposed in Fig. 3. For phyllosilicates containing cobalt an increase of the lamellar distance occurred, to give the values of 1811 pm for SILMg1/ $\text{Co}^{2+}$  and 2235 pm for SILMg2/ $\text{Co}^{2+}$ . This behaviour seems to be related to the low amount of cation inserted, as compared with other cations, as shown in Table 2. However, in these diffractograms a peak related to the 060 plane, corresponding to a distance of 157.5 pm, is characteristic for trioctahedral phyllosilicates<sup>18-20</sup> and was maintained in the final adsorbed nanocomposites.

The ability of this material to extract cations was confirmed by the adsorption isotherms shown in Fig. 4. The  $N_f$  value was calculated by applying the expression  $N_f = (N_i - N_s)m^{-1}$ , where  $N_i$  and  $N_s$  are the numbers of moles of cations added to the

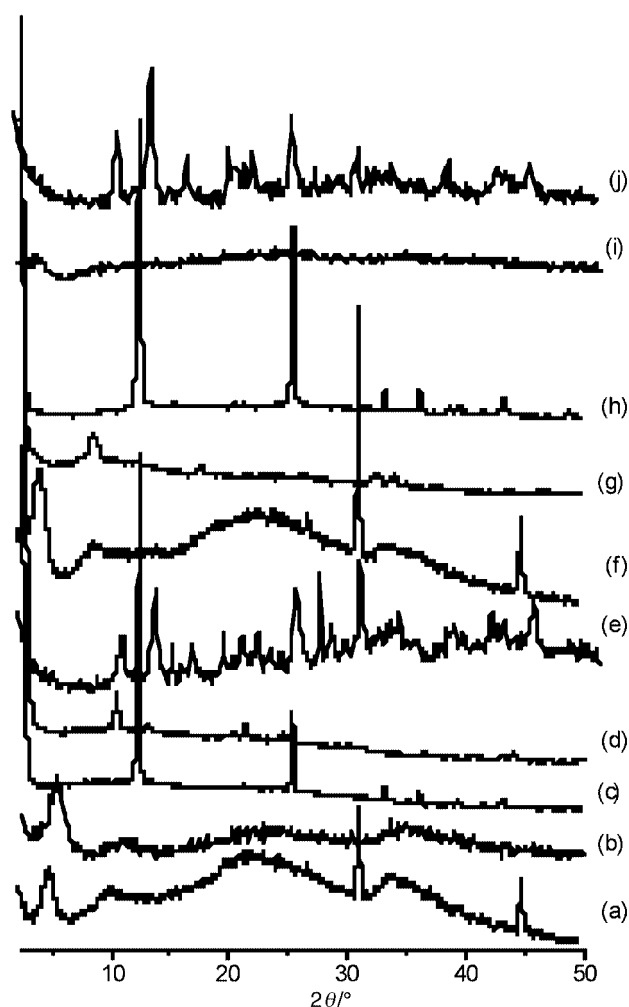


**Fig. 2** Comparative XRD patterns for (a) SILMg1, (b) SILMg1/ $\text{Co}^{2+}$ , (c) SILMg1/ $\text{Cu}^{2+}$ , (d) SILMg1/ $\text{Zn}^{2+}$ , (e) SILMg1/ $\text{Ni}^{2+}$ , (f) SILMg2, (g) SILMg2/ $\text{Zn}^{2+}$ , (h) SILMg2/ $\text{Cu}^{2+}$ , (i) SILMg2/ $\text{Co}^{2+}$  and (j) SILMg2/ $\text{Ni}^{2+}$ .

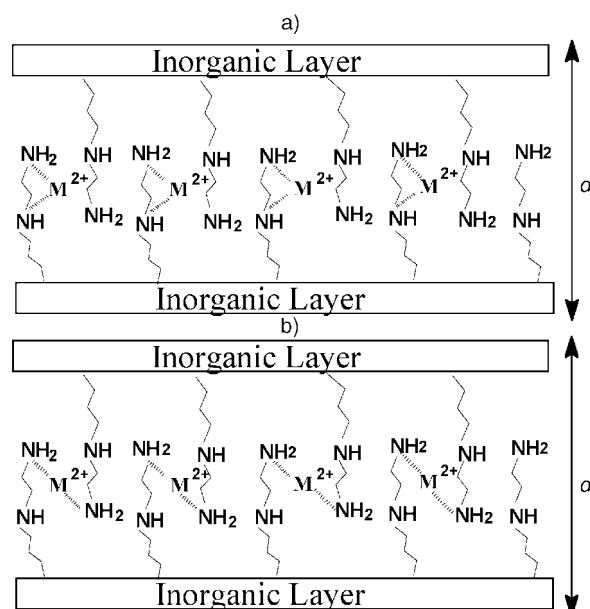


**Fig. 3** Proposed complexed structure upon metal adsorption in the gallery space of the modified phyllosilicate.

system and at equilibrium in solution, and  $m$  is the mass of the hybrid used in grams for each assay. The general representation of the adsorption process is given by reaction (1).

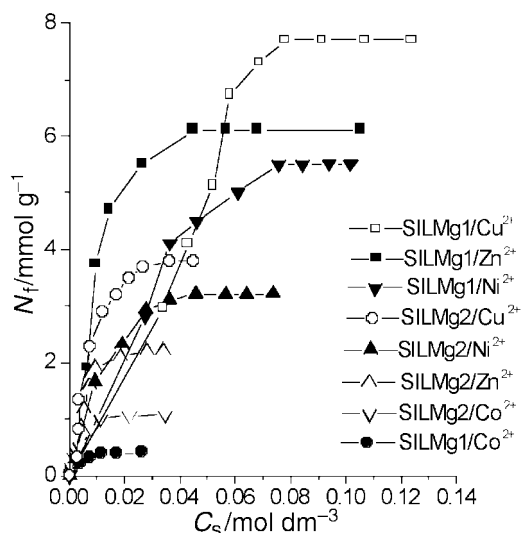


**Fig. 4** Adsorption isotherms of cations on SILMg1 and SILMg2. The scale of the concentration  $C_s$  for cobalt cation in both phyllosilicates was multiplied by 10.

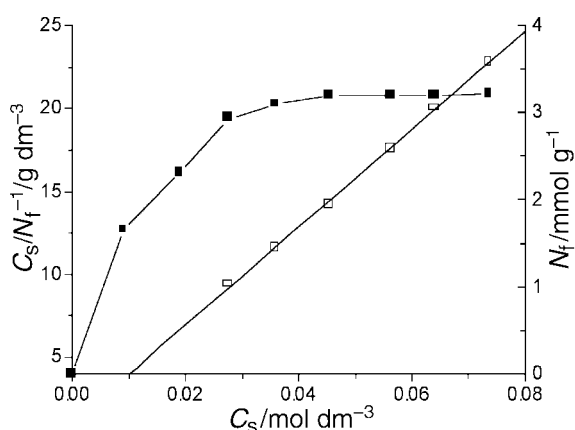
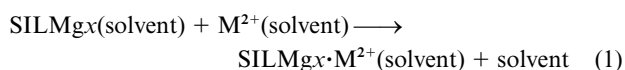


**Fig. 5** Adsorption isotherm of  $\text{Ni}^{2+}$  on SILMg2 and its linearization.



For these adsorptions the modified Langmuir equation (2) can

$$\frac{C_s}{N_f} = \frac{1}{(N_s b)} + \frac{C_s}{N_s} \quad (2)$$

be applied, where  $C_s$  is the concentration of the cations ( $\text{mol dm}^{-3}$ ) remaining in solution after reaching equilibrium in the solid-liquid interface,  $N_f$  is defined as previously ( $\text{mol g}^{-1}$ ),  $N_s$  is the maximum amount of solute per gram of adsorbent ( $\text{mol g}^{-1}$ ), which depends on the number of adsorption sites and, therefore, is related to the intensity of the adsorption and  $b$  is a constant. A plot of  $C_s/N_f$  against  $C_s$  allows the determination of the constants  $N_s$  and  $b$ , as illustrated in Fig. 5. This proposed model assumes that all the species in equilibrium at very dilute solution behave ideally, where the solute and the solvent occupy the same areas in the monolayer in a homogeneous surface.<sup>21</sup> The results are presented in Table 2.

As observed, the  $N_s$  values follow the same order as obtained by the adsorption isotherm and differ only a little from the  $N_f$  values, with the exception of copper whose  $N_s$  values are greater than those obtained experimentally. This value shows that the adsorption capacity is larger than the observed adsorption for that cation. The values of the coefficient of correlation also indicated a reasonable adjustment of the data to the Langmuir model. The increasing order of adsorption was  $\text{Cu}^{2+} < \text{Zn}^{2+} <$

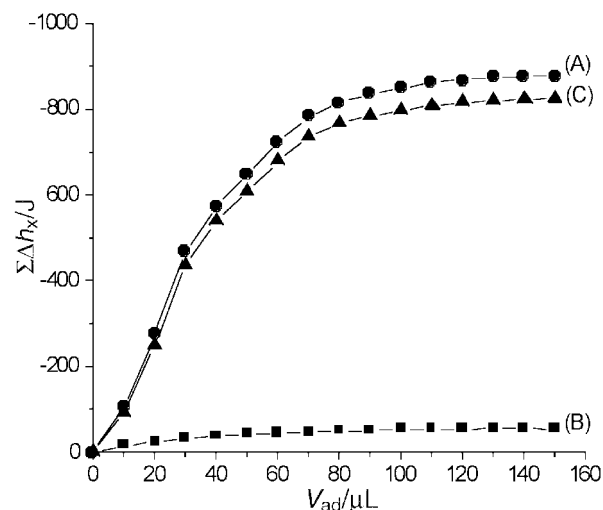


**Fig. 6** Calorimetric titration of a suspension of 0.0163 g of SILMg1 in 2.0  $\text{cm}^3$  of water with  $1.03 \text{ mol dm}^{-3}$   $\text{Zn}(\text{NO}_3)_2$  in the same solvent at  $298.15 \pm 0.02 \text{ K}$ . The experimental points in curves A, B and C represent the sum of the thermal effects of the cation titration ( $\Sigma\Delta h_{\text{tit}}$ ), cation dilution ( $\Sigma\Delta h_{\text{dil}}$ ) and the net thermal effect of adsorption ( $\Sigma\Delta h_r$ ), respectively.

$\text{Ni}^{2+} < \text{Co}^{2+}$  for SILMg1 and  $\text{Cu}^{2+} < \text{Ni}^{2+} < \text{Zn}^{2+} < \text{Co}^{2+}$  for SILMg2. For a given cation the adsorption capacity is larger for SILMg1. This behaviour can be justified by the fact that in SILMg1 there is a larger space between the pendant groups to favour the interaction with metallic cations, to form monodentate complexes. However, for SILMg2 there are two possibilities of co-ordination: the cation is mono- or bi-dentate complexed by the basic centres of the pendant groups, as shown in Fig. 3.

The experimental order obtained for the  $N_s$  values did not correlate with the values of the volume of hydration ( $\text{cm}^3 \text{ mol}^{-1}$ ) for the cations as shown by the sequence for divalent cations (volume):  $\text{Cu} (147.8) = \text{Ni} (147.8) < \text{Co} (169.6) < \text{Zn} (178.2)$ .<sup>22-24</sup> The small volumes of hydration displayed by copper and nickel make it easier to access the interlamellar positions. On the contrary, the volume of zinc is prone to give it the largest hindrance to the basic centres within the lamella.

The calorimetric titration investigation supplied a larger amount of information on the processes of the interaction of the cations with the basic centres of the nanocomposites. Fig. 6 illustrates the calorimetric titration of an aqueous solution of zinc on phyllosilicate SILMg1, where the integral thermal effects of the interaction ( $\Sigma\Delta h_{\text{int}}$ ), the dilution of the metal ion solution ( $\Sigma\Delta h_{\text{dil}}$ ) and that of the interaction ( $\Sigma\Delta h_r$ ) were determined. The enthalpy of adsorption and the concentration of the metal ion at equilibrium are related by expression (3)<sup>25-28</sup> where  $\Sigma X$  is the molar fraction of the cation in solution

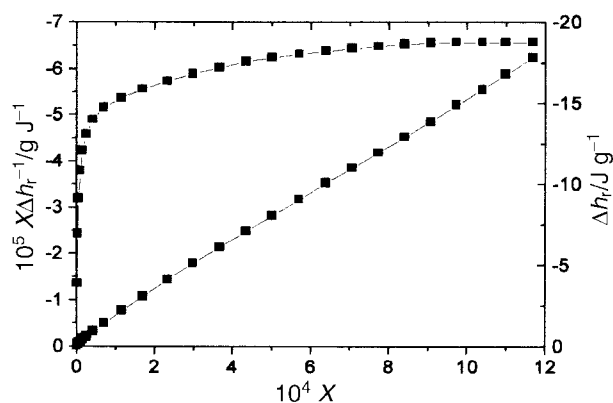
$$\frac{\Sigma X}{\Sigma\Delta h_r} = \frac{1}{[(K-1)\Delta h_{\text{mono}}]} + \frac{\Sigma X}{\Delta h_{\text{mono}}} \quad (3)$$

at equilibrium,  $\Sigma\Delta h_r$  the integral enthalpy of the adsorption,  $K$  a proportionality factor that includes the equilibrium constant and  $\Delta h_{\text{mono}}$  is the enthalpy of adsorption for the formation of the monolayer.

A plot of  $\Sigma\Delta h_r$  against  $X$  gives the calorimetric curve of the process and its linearization allows the determination of  $\Delta h_{\text{mono}}$  from the angular coefficient of the straight line. Fig. 7 shows this for nickel adsorbed on SILMg1 hybrid. The molar enthalpy of interaction can be determined through the equation  $\Delta H = \Delta h_{\text{mono}} (N_{\text{int}})^{-1}$ . For the obtained values of  $K$ , the free energy of the process was calculated through  $\Delta G = -RT \ln K$  and also the molar entropy by combining  $\Delta H$  and  $\Delta G$  values, by using the expression  $\Delta G = \Delta H - T\Delta S$ . These data are listed in Table 3.

**Table 3** Thermodynamic values for adsorption of metal cations on SILMg1 and SILMg2 nanocomposites

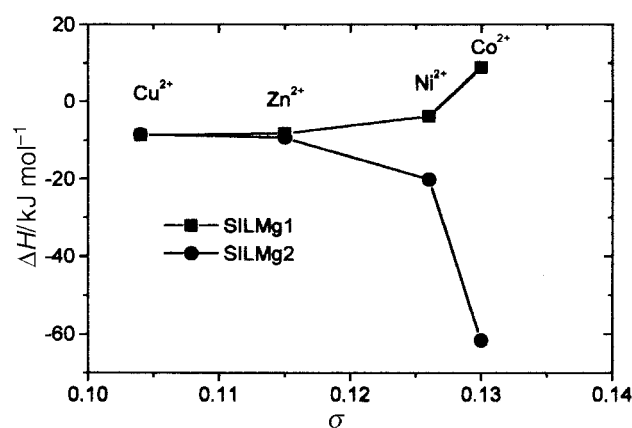
Hybrid	M <sup>2+</sup>	−Δ <i>h</i> <sub>int</sub> /J g <sup>−1</sup>	−Δ <i>H</i> /kJ mol <sup>−1</sup>	−Δ <i>G</i> /kJ mol <sup>−1</sup>	Δ <i>S</i> /J K <sup>−1</sup> mol <sup>−1</sup>
SILMg1	Cu <sup>2+</sup>	66.62 ± 0.37	8.62 ± 0.56	23.4 ± 0.2	50 ± 3
	Zn <sup>2+</sup>	50.28 ± 0.44	8.20 ± 0.48	24.3 ± 0.3	54 ± 3
	Ni <sup>2+</sup>	20.81 ± 0.10	3.78 ± 0.03	26.8 ± 0.4	77 ± 1
	Co <sup>2+</sup>	−3.60 ± 0.01	−8.86 ± 0.81	33.7 ± 0.3	143 ± 4
SILMg2	Cu <sup>2+</sup>	35.10 ± 0.04	8.40 ± 0.50	30.4 ± 0.6	74 ± 3
	Zn <sup>2+</sup>	19.04 ± 0.26	9.29 ± 0.55	30.6 ± 0.5	63 ± 3
	Ni <sup>2+</sup>	64.18 ± 0.17	20.12 ± 0.67	28.2 ± 0.3	27 ± 3
	Co <sup>2+</sup>	73.86 ± 0.20	61.55 ± 0.06	31.5 ± 0.3	101 ± 1

**Fig. 7** Isotherm for the integral enthalpy of adsorption ( $\Sigma\Delta h_i$ ) versus molar fraction ( $\Sigma X$ ) obtained from a calorimetric titration of a suspension of 0.01568 g of SILMg1, in 2.0 cm<sup>3</sup> of water, with 1.06 mol dm<sup>−3</sup> Ni(NO<sub>3</sub>)<sub>2</sub> in the same solvent at 298.15 ± 0.02 K. The straight line is the linearized form of the isotherm.

As observed, with the exception of Co<sup>2+</sup> on SILMg1 hybrid, the enthalpy values for the interactive processes are exothermic in nature. Based on the sequence of the enthalpic values, the order Cu<sup>2+</sup> > Zn<sup>2+</sup> > Ni<sup>2+</sup> > Co<sup>2+</sup> was established for SILMg1, however an opposite order was found for SILMg2.

The variation in entropy gave positive values, which are associated to a disorder of the arrangement of molecules of the solvents in the final adsorption stage of the system, consistent with the favourable occurrence of these reactions.<sup>27</sup> This entropic effect can be explained by the fact that during the adsorption processes cations lose molecules of water of hydration to the environment. On the other hand, molecules of water hydrogen bonded to the aminated chains are also lost during co-ordination. This transference of water molecules to the bulk promotes a disturbance in the medium, causing an increase in entropy.

The variations of free energy are all favourable, following the same enthalpic order in values for SILMg1 and, with the exception of Ni<sup>2+</sup>, all free energy values are very similar to those for SILMg2. With the exception of cobalt, all Δ*G* values are largest for SILMg2. This fact might be related to the bidentate complexes formed with this hybrid, enhancing the stability of the final compound due to an acid–base interaction, as described by Pearson's softness parameter ( $\sigma$ ) for acidity to the metal.<sup>29</sup> The  $\sigma$  values decrease with increasing softness of the corresponding cation in aqueous systems. An interesting correlation was obtained by considering the thermochemical data and the reactivity of the metallic cations expressed by Pearson's parameter. Thus, the  $\sigma$  values for divalent cations of copper, zinc, nickel and cobalt are 0.104, 0.115, 0.126 and 0.130, respectively.<sup>29</sup> Then, the hardness of the acid follows the order Co<sup>2+</sup> > Ni<sup>2+</sup> > Zn<sup>2+</sup> > Cu<sup>2+</sup>. This sequence is the same as obtained for the enthalpy of the reactions with SILMg2 hybrid but inverse in relation to the order found with SILMg1. An illustration of this behaviour is presented in Fig. 8, which shows that copper and zinc are disposed on the same straight line, while nickel and cobalt are located in antagonistic positions in

**Fig. 8** Comparison between enthalpic values  $\Delta H$  and Pearson's parameter  $\sigma$  of metallic cations on SILMg1 and SILMg2 systems.

relation to the preceding cations. These values suggest that the type of interaction involving nickel and cobalt differs from the one involving copper and zinc, reflecting the enthalpic values found for both inorganic–organic hybrids. Based on these values, it seems that the interlamellar complex formed in SILMg2/Ni<sup>2+</sup> and SILMg2/Co<sup>2+</sup> hybrids is favoured due to the larger amount of hard basic centres. Therefore, nickel and cobalt cations have a preference for reacting with the aminated groups, to give exothermic values. The smaller amount of basic centres on SILMg1 resulted in the formation of a monodentate complex, and in a less intense reaction than on SILMg2 hybrid.

### Acknowledgements

The authors are indebted to CAPES/PICD/UEPB and CNPq for fellowships and to FAPESP for financial support.

### References

- 1 T. J. Pinnavaia, *Science*, 1983, **220**, 4595.
- 2 T. Mizutani, Y. Fukushima, A. Okada and O. Kamigaito, *Bull. Chem. Soc. Jpn.*, 1990, **63**, 2094.
- 3 Y. Fukushima and M. Tami, *J. Chem. Soc., Chem. Commun.*, 1995, 24.
- 4 Y. Fukushima and M. Tami, *Bull. Chem. Soc. Jpn.*, 1996, **69**, 3667.
- 5 S. L. Burkett, A. Press and S. Mann, *Chem. Mater.*, 1997, **9**, 1071.
- 6 Y.-S. Hong and S.-J. Kim, *Bull. Korean Chem. Soc.*, 1997, **18**, 2.
- 7 N. T. Whilton, S. L. Burkett and S. Mann, *J. Mater. Chem.*, 1998, **8**, 1927.
- 8 T. P. Lishko, L. V. Glushchenko, Y. V. Kholin, Z. N. Zaitsev, A. Bugaevskii and N. D. Donskaya, *Russ. J. Phys. Chem.*, 1991, **65**, 1584.
- 9 A. R. Cestari and C. Airoidi, *J. Colloid Interface Sci.*, 1997, **195**, 338.
- 10 A. R. Cestari and C. Airoidi, *Colloids Surf. A*, 1996, **117**, 7.
- 11 E. F. S. Vieira, J. A. Simoni and C. Airoidi, *J. Mater. Chem.*, 1997, **7**, 11.
- 12 S. Roca and C. Airoidi, *Thermochim. Acta*, 1996, **284**, 289.
- 13 K. Nakamoto, *Infrared Spectra of Inorganic and Co-ordination Compounds*, 2nd edn., Wiley-Interscience, New York, 1970.
- 14 R. M. Silverstein, G. C. Bassler and T. C. Morrel, *Spectrometric Identification of Organic Compounds*, Wiley, Singapore, 1991.

- 15 D. L. Pavia, G. M. Lampman and G. S. Kriz, *Introduction to Spectroscopy*, 2nd edn., Saunders College Publishing, New York, 1996.
- 16 K. A. Carrado and L. Xu, *Microporous Mesoporous Mater.*, 1999, **27**, 87.
- 17 M. G. Fonseca, C. R. Silva and C. Airoidi, *Langmuir*, 1999, **15**, 5048.
- 18 J. H. Rayner and G. Brown, *Clays Clay Miner.*, 1973, **21**, 103.
- 19 D. M. Moore and R. C. Reynolds, *X-Ray Diffraction and the Identification and Analysis of Clay Minerals*, Oxford University Press, London, 1997.
- 20 G. W. Brindely and G. Brown, *Crystal Structures of Clay Minerals and their X-Ray Identification*, 1st edn., Mineralogical Society, London, 1980.
- 21 A. W. Adamson, *Physical Chemistry of Surfaces*, 5th edn., Wiley, New York, 1990.
- 22 G. Krestov, *Thermodynamics of Solvation: Solution and Dissolution; Ions and Solvents; Structure and Energetics*, 1st edn., Ellis Horwood, London, 1991.
- 23 Y. Marcus, *Ion Solvation*, Wiley, London, 1985.
- 24 A. Bem-Naim, *Solvation Thermodynamics*, Plenum, New York, 1987.
- 25 R. M. C. Santos and C. Airoidi, *J. Mater. Chem.*, 1994, **4**, 1479.
- 26 C. Airoidi and E. F. C. Alcântara, *J. Chem. Thermodyn.*, 1995, **27**, 623.
- 27 S. Roca and C. Airoidi, *J. Chem. Soc., Dalton Trans.*, 1997, 2517.
- 28 C. Airoidi and E. F. C. Alcântara, *Thermochim. Acta*, 1995, **259**, 95.
- 29 S. J. Ashcroft and G. Beech, *Inorganic Thermodynamics*, Pitman Press, London, 1973.

Paper 9/05733A